The Bayesian analysis of the backreaction models

Krzysztof Bolejko[1,2], **Aleksandra Kurek**[3] **and Marek Szydłowski**[4,5]

[1]School of Physics, University of Melbourne, VIC 3010, Australia

[2]Nicolaus Copernicus Astronomical Center, Bartycka 18, 00-716 Warsaw, Poland

[3]Astronomical Observatory, Jagiellonian University, Orla 171, 30-244 Kraków, Poland

[4]Mark Kac Complex Systems Research Centre, Jagiellonian University, Reymonta 4, 30-059 Kraków, Poland

[5]Department of Theoretical Physics, Faculty of Philosophy, The John Paul II Catholic University of Lublin, Al. Racławickie 14, 20-950 Lublin, Poland

E-mail: `bolejko@camk.edu.pl`, `alex@oa.uj.edu.pl`, `uoszydlo@cyf-kr.edu.pl`

Abstract. We present the Bayesian analysis of four different type of backreaction models. These backreaction models are based on the Buchert equations. In this approach one considers a solution to the Einstein equations for a general matter distribution and then an average of various observable quantities is taken. Such an approach has become of considerable interest when it was shown that it can lead to an agreement with observations without resorting to dark energy.

In this paper we test the models with supernovae, BAO, and CMB data. The results favour the ΛCDM model over the backreaction models which were tested in the paper. However, the tested models were based on some particular assumptions about the relation between the average spatial curvature and the backreaction as well as the relation between the curvature and curvature index. In this paper we modified the latter assumption leaving the former unchanged. We found that by varying the relation between the curvature and curvature index we can obtain a better fit. Thus, some further work is still needed, especially the relation between the backreaction and the curvature should be revisited in order to fully determine the feasibility of the backreaction models to mimic dark energy.

1. Introduction

The Universe, as observed, is almost on all scales very inhomogeneous. However, in standard approach to cosmology, it is assumed that the Universe can be described by the homogeneous and isotropic Friedmann–Lemaître–Robertson–Walker (FLRW) models. The FLRW models provide a remarkably precise description of cosmological observations but to achieve this we need to pay one price – in order to obtain the concordance with observations it needs to be assumed that the Universe is filled with an unknown substance called dark energy. However, this substance has never been observed directly and since it has very unusual properties some began to ask whether dark energy is real or if it is the description of the Universe which requires the existence of such an exotic entity that is invalid.

While it is possible that our Universe is filled with dark energy many alternatives has been already proposed: brane-world cosmologies (see [1] for a review), f(R) cosmology (see [2] for a review), application of inhomogeneous cosmological models (for a review see [3]) and others. One of recently proposed approaches is based on an averaging framework. Such approach is motivated by the fact that the Einstein equations are not linear, which means that the solution of the Einstein equations for a homogeneous matter distribution is different than the averaged solution to the Einstein equations for a general matter distribution. In other words, the evolution of the homogeneous model might be slightly different from the evolution of an inhomogeneous Universe, even though inhomogeneities in the Universe when averaged over a sufficiently large scale might tend to be zero. The difference between the evolutions of a homogeneous and inhomogeneous models of the Universe is known as the backreaction effect. In this approach, one considers a solution to the Einstein equations for a general matter distribution and then an average of various observable quantities is taken. Under a certain assumptions such an attempt leads to the Buchert equations [6]. The Buchert equations are very similar to the Friedmann equations except for the backreaction term which is in general non vanishing, if inhomogeneities are present. For a review on the backreaction effect and the Buchert averaging scheme the reader is referred to [7, 8, 9]. Based on this scheme Larena et al. have recently proposed a model [10], where the metric of the Universe at a given instant looks like the FLRW metric, but the evolution of the scale factor is governed by the Buchert equations. In this paper we aim to perform the Bayesian analysis of the cosmological observations within the models proposed in [10].

2. Homogeneous-like universe evolving inhomogeneously

If the averaging procedure is applied to the Einstein equations, then for irrotational, pressureless matter and 3+1 ADM space-time foliation with a constant lapse and a vanishing shift vector, the following equations are obtained [6]

$$3\frac{\ddot{a}}{a} = -4\pi G\langle\rho\rangle + \mathcal{Q}, \tag{1}$$

$$3\frac{\dot{a}^2}{a^2} = 8\pi G\langle\rho\rangle - \frac{1}{2}\langle\mathcal{R}\rangle - \frac{1}{2}\mathcal{Q}, \tag{2}$$

$$\mathcal{Q} \equiv \frac{2}{3}\left(\langle\Theta^2\rangle - \langle\Theta\rangle^2\right) - 2\langle\sigma^2\rangle, \tag{3}$$

where a dot ($\dot{}$) denotes ∂_t, $\langle\mathcal{R}\rangle$ is an average of the spacial Ricci scalar ${}^{(3)}\mathcal{R}$, Θ is the scalar of expansion, σ is the shear scalar, and $\langle\ \rangle$ is the volume average over the hypersurface of constant time: $\langle A\rangle = (\int d^3x\sqrt{-h})^{-1}\int d^3x\sqrt{-h}A$, and the scale factor a

is defined as a cube root of the volume:

$$a = \left(\frac{V}{V_0}\right)^{1/3}, \tag{4}$$

where V_0 is an initial volume.

Equation (1) is compatible with (2) if the following integrability condition holds

$$\frac{1}{a^6}\partial_t\left(\mathcal{Q}a^6\right) + \frac{1}{a^2}\partial_t\left(\langle R\rangle a^2\right) = 0. \tag{5}$$

Similarly as in the FLRW models the following parameters can be introduced:

$$H = \frac{\dot{a}}{a}, \quad \Omega_m = \frac{8\pi G}{3H^2}\langle\rho\rangle, \quad \Omega_{\mathcal{R}} = -\frac{\langle\mathcal{R}\rangle}{6H^2}, \quad \Omega_{\mathcal{Q}} = -\frac{\langle\mathcal{Q}\rangle}{6H^2}. \tag{6}$$

The Hamiltonian constrains, can then be written as:

$$\Omega_m + \Omega_{\mathcal{R}} + \Omega_{\mathcal{Q}} = 1. \tag{7}$$

As can be seen $\Omega_{\mathcal{R}} + \Omega_{\mathcal{Q}}$ can act like Ω_Λ. Moreover, if the dispersion of the expansion is large then $\mathcal{Q}$ can be large and as seen from (3), one can get acceleration ($\ddot{a} > 0$) without the need for dark energy.

The template metric of the Universe - the metric which describes the averaged universe can be written as

$$\mathrm{d}s^2 = \mathrm{d}t^2 - \frac{a(t)^2}{1-k(t)r^2}\mathrm{d}r^2 - a(t)^2r^2\left(\mathrm{d}\vartheta^2 + \sin^2\vartheta\mathrm{d}\varphi^2\right). \tag{8}$$

A similar approach, i.e. to consider the template metric with the scale factor which evolves accordingly to the Buchert equations instead of the Friedmann equations was first introduced by Paranjape and Singh [12], though in their model k was constant. The motivation for $k(t)$ comes from the fact that the averaged spatial curvature if calculated at one instant does not have to be the same as the averaged spatial curvature calculated at another instant.

The Buchert equations do not form a closed system. To close these equations, and thus to calculate the evolution of the scale factor one has to introduce some further assumptions [6]. One of such assumptions can be: $\langle\mathcal{R}\rangle \sim \mathcal{Q}$ [10]. As seen from the integrability condition (5) this leads to

$$\langle\mathcal{R}\rangle = \langle\mathcal{R}\rangle_i a^n \quad \text{and} \quad \mathcal{Q} = -\frac{n+2}{n+6}\langle\mathcal{R}\rangle_i a^n. \tag{9}$$

Now, the final step is to derive a relation between the average spacial curvature $\langle\mathcal{R}\rangle$ and the curvature index k. In analogy to the FLRW models the following relation can be proposed [10]:

$$k = \frac{a^2\langle\mathcal{R}\rangle}{a_i^2|\langle\mathcal{R}\rangle_i|}, \quad \rightarrow \quad k(z) = -\frac{(n+6)(1-\Omega_m)(1+z)^{-(n+2)}}{|(n+6)(1-\Omega_m)|}. \tag{10}$$

In Sec. 3.2.2 we will modify the above assumption and test models with different relations between k and $\langle\mathcal{R}\rangle$. Summarising, the model considered in this paper is described by the metric (8), but the evolution of the scale factor is governed by the Buchert equations. Employing the assumptions (9) and (10) the evolution equations reduce to the following relation:

$$H = H_0\sqrt{\Omega_m(1+z)^3 + (1-\Omega_m)(1+z)^{-n}}. \tag{11}$$

As seen, this model is parametrised by two parameters: Ω_m and n. The distance, using (8), can be then calculated by solving

$$\frac{dr}{dz} = \sqrt{\frac{1-kr^2}{\Omega_m(1+z)^3 + (1-\Omega_m)(1+z)^{-n}}}. \tag{12}$$

Larena et al. [10] tested this model with the likelihood analysis using the supernova and CMB data. They found that this model is in the agreement with observations. In next section we will perform the Bayesian analysis of this model using the supernova data, baryon acoustic oscillations (BAO) and the observation of the cosmic microwave background (CMB) radiation.

3. Bayesian analysis

The model presented in the preceding section will be confronted with cosmological observations in the Bayesian framework using the CosmoNest code [15] ‡ which was adapted to our case. In the Bayes Theory all what we know about the vector of parameters ($\bar{\theta}$) of a given model (M) is contained in the posterior probability density function (PDF), which is given by

$$P(\bar{\theta}|D,M) = \frac{P(D|\bar{\theta},M)P(\bar{\theta}|M)}{P(M|D)}, \tag{13}$$

where D denotes the set of data used in analysis; $P(D|\bar{\theta},M)$ is the likelihood function for a given model and in the rest part of the paper will be referred to as $L(\bar{\theta})$; $P(\bar{\theta}|M)$ is the prior PDF, which enables us to include our previous knowledge (i.e. without information coming from the data D) about parameters under consideration; the last quantity $P(M|D)$ is the normalization constant, called the evidence (or marginal likelihood) and is the most important quantity in the Bayesian framework of model comparison. The posterior PDF could be simply summarize in terms of a best fit value, which could be the posterior PDF mode (the most probable value of $\bar{\theta}$) or the mean of the marginal posterior PDF of a given parameter (θ_i), which is obtained by integration (13) over remaining parameters.

‡ The CosmoNest code uses the nested sampling algorithm [16] and is a part of the CosmoMC code [17].

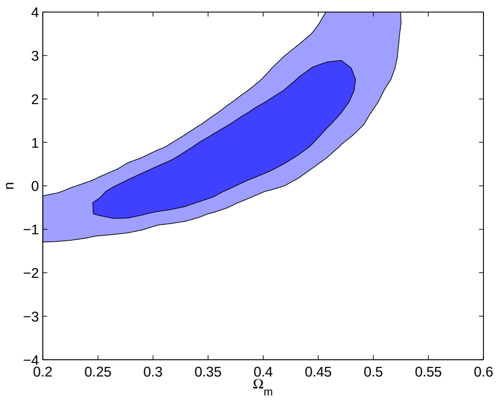

Figure 1. Constraints from SN data (SNLS - left panel, Union - right panel).

3.1. Parameters estimation

3.1.1. Supernova data

Firstly, we consider observations of Type-Ia supernova, which are taken from the Supernova Legacy Survey [18] and the Union Supernova Compilation [19]. After analytical marginalization over the H_0 parameter the likelihood function is of the following form

$$L_{SN}(\Omega_m, n) \propto \exp\left[-\frac{1}{2}\left(\sum_{i=1}^{N}\frac{x_i^2}{\sigma_i^2} - \frac{\left(\sum_{i=1}^{N}\frac{x_i}{\sigma_i^2}\right)^2}{\sum_{i=1}^{N}\frac{1}{\sigma_i^2}}\right)\right], \tag{14}$$

where N is the number of data ($N = 115$ for SNLS sample and $N = 307$ for Union sample), σ_i is an observational error, $x_i = \mu_i^{\text{theor}} - \mu_i^{\text{obs}}$, $\mu_i^{\text{obs}} = m_i - M$ (m_i–apparent magnitude, M–absolute magnitude of SNIa) is the observed distance moduli, and $\mu_i^{\text{theor}} = 5\log_{10} D_L + 25$, where $D_L = cr(1+z)$ is the luminosity distance, and r is given by (12).

We assume a flat prior PDF for the model parameters in the following ranges: $\Omega_m \in [0.2, 0.6]$ and $n \in [-4, 4]$. The 68% and 95% contours of the posterior PDF for the SNLS and Union sample are presented in Fig. 1.

3.1.2. CMB data

The second set of cosmological observations comprise measurement of the CMB angular power spectrum. If it is assumed that the early Universe (before and up to the last scattering instant) is well described by the FLRW model then the CMB power spectrum can be parametrized by [20]

$$l_m = l_a(m - \phi_m), \tag{15}$$

where l_1, l_2, l_3 is a position of the first, second and third peak, and

$$l_a = \pi\frac{r_*}{r_s}, \tag{16}$$

where r_* is a co-moving distance to the last scattering surface and r_s is a size of the sound horizon at the last scattering instant. The function ϕ_m describes the phase shift of the m-th peak and is sensitive mainly to the pre-recombination physics. It depends on the baryon density ($\Omega_b h^2$), where $h = H_0/(100 \text{ Mpc km s}^{-1})$, on the ratio of the radiation to matter density at last scattering [$\rho_r(z_*)/\rho_m(z_*) = 0.042(\Omega_m h^2)^{-1}(z_*/10^3)$], where z_* is the recombination redshift, on the spectral index (n_s), and on the density of the dark energy before recombination.

We fit the position of the first and second peak and the first trough of the CMB power spectrum [21]. We assume that $n_s = 1$ and neglect the density of dark energy before recombination. $r_* = c/H_0 r(z_*)$ and $r(z)$ is given by (12) and $r_s = c(2/3k_{eq})\sqrt{6/R_{eq}}\ln[(\sqrt{1+R_*}+\sqrt{R_*+R_{eq}})/(1+\sqrt{R_{eq}})]$, where $R_{eq} = R/(1+z_{eq})$, $R_* = R/(1+z_*)$, $k_{eq} = H_0\sqrt{2\Omega_m z_{eq}}$, $R = 31500\Omega_b h^2(T_{CMB}/2.7K)^{-4}$ and $z_{eq} = 2.5\times10^4\Omega_m h^2(T_{CMB}/2.7K)^{-4}$. We take $T_{CMB} = 2.728$ and employ the fitting formulae for z_* as provided in Ref. [22].

The likelihood function is of the following form

$$L_{CMB}(\Omega_m, n, \Omega_b h^2, h) \propto \exp\left[-\frac{1}{2}\left(\left(\frac{l_1 - 220.8}{0.7}\right)^2 + \left(\frac{l_{3/2} - 412.4}{1.9}\right)^2 + \left(\frac{l_2 - 530.9}{3.8}\right)^2\right)\right]. \quad (17)$$

We assume a flat prior PDF for the model parameters in the ranges: $\Omega_m \in [0.2, 0.6]$, $n \in [-4, 4]$, $h \in [0.64, 0.80]$ (using information from HST [23]), $\Omega_b h^2 \in [0.0203, 0.0223]$ (using information from BBN [24]).

The 68% and 95% contours of posterior PDF (after marginalization over h and $\Omega_b h^2$) obtained in the analysis with the CMB data as well as in the analysis with the joint data set (SNIa+CMB) (here the likelihood function has the following form $L = L_{SN}L_{CMB}$) are presented in Fig. 2.

The posterior mode is: $\Omega_m = 0.32$, $n = 0.00$, $h = 0.79$, $\Omega_b h^2 = 0.0223$ for the SNLS+CMB data set and $\Omega_m = 0.36$, $n = 0.35$, $h = 0.76$, $\Omega_b h^2 = 0.0223$ for the Union+CMB data set. The mean of the marginal posterior PDF for the given parameter (presented in Fig. 3), together with the 68% Bayesian confidence interval (credible interval) are gathered in Table 1 and Table 2 for SNLS+CMB and Union+CMB respectively.

3.1.3. BAO data

In addition to the geometric measurements described above, we study constraints obtained from the measured dilation scale of the BAO in the redshift space power-spectrum of 46,748 luminous red galaxies (LRG) from the Sloan Digital Sky Survey (SDSS). The dilation scale is defined as

$$D_V = \left[D_A^2 \frac{cz}{H(z)}\right]^{1/3}, \quad (18)$$

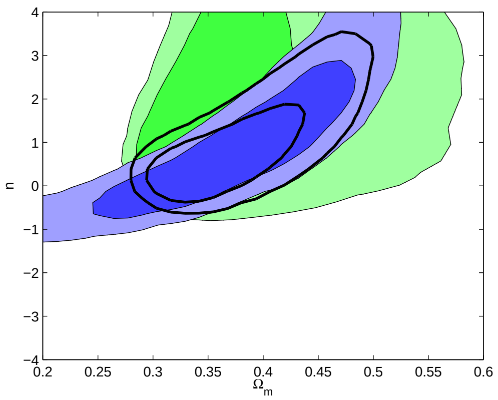

Figure 2. Constraints from SN (blue), CMB (green) and SN+CMB (black) data (SNLS+CMB - left panel, Union+CMB - right panel).

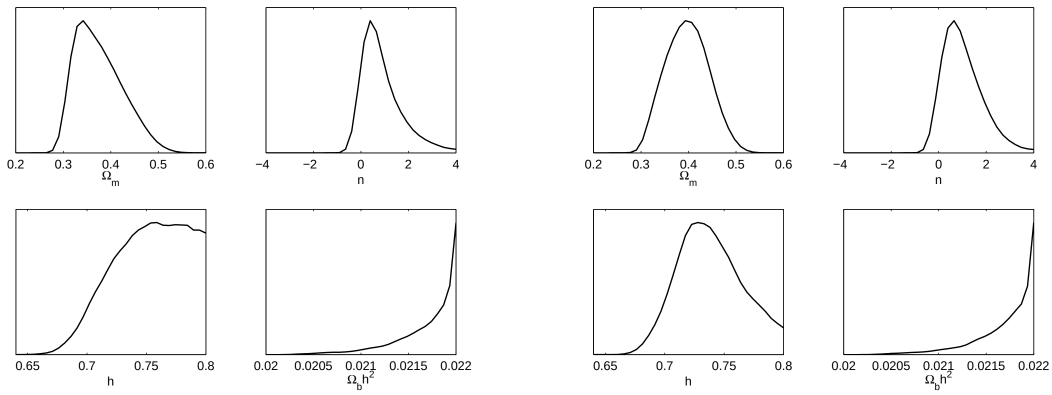

Figure 3. Marginal posterior PDF for model parameters (SNLS+CMB - left panel, Union+CMB - right panel.

where D_A is the co-moving angular diameter distance and $H(z)$ is the Hubble parameter in function of redshift. The measured value of the dilation scale at $z = 0.35$ is 1370 ± 64 Mpc. It should be noted that the value of 1370 ± 64 Mpc was obtained within the framework of the linear perturbations imposed on the homogeneous FLRW background. Instead, such analysis should be carried out within the framework of the model considered in this paper. Otherwise, we should be aware of possible systematical errors. When the geometry of the space time is not FLRW the possible sources of errors are: (1) the sound horizon can be distorted and can be of different size in parallel and perpendicular direction; (2) the expansion rate can be of different value with respect to parallel and perpendicular direction; (3) the redshift distortions if analysed within the inhomogeneous model, might lead to estimates different from those received within the standard approach; (4) another source of error comes from the fact that in their analysis Eisenstein et al. converted redshift of LRG galaxies to a distance assuming the ΛCDM

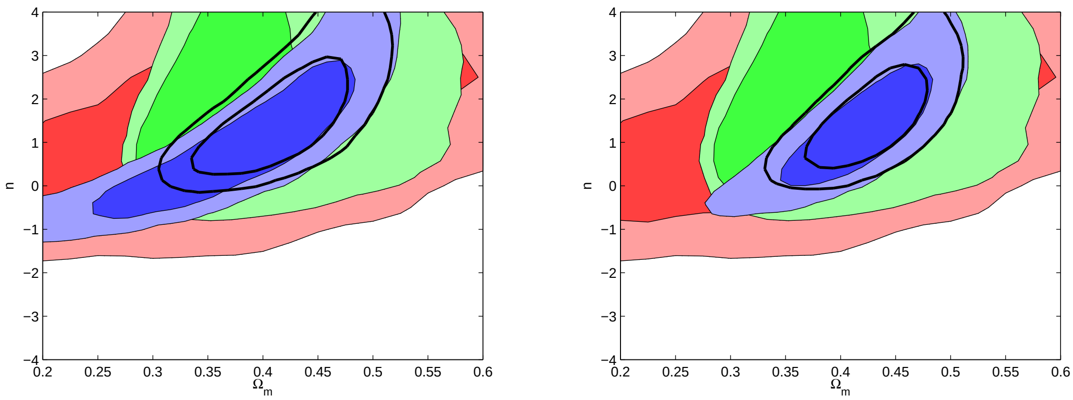

Figure 4. Constraints from SNIa (blue), CMB (green), BAO (red) and SNIa+CMB+BAO (black) data sets (SNLS+CMB+BAO - left panel, Union+CMB+BAO - right panel).

Table 1. Mean of the marginal posterior PDF for the model parameters together with the 68% credible interval for the SNIa+CMB and SNIa+CMB+BAO data sets.

	SNLS+CMB	SNLS+CMB+BAO
Ω_m	$0.37^{+0.06}_{-0.04}$	$0.42^{+0.04}_{-0.05}$
n	$0.87^{+0.78}_{-0.71}$	$1.59^{+0.91}_{-0.85}$
h	$0.75^{+0.03}_{-0.03}$	$0.73^{+0.02}_{-0.03}$
$\Omega_b h^2$	$0.0219^{+0.0003}_{-0.0003}$	$0.0219^{+0.0003}_{-0.0003}$

model. Despite these uncertainties we proceed with the analysis to see how the BAO data can possibly constrain the data. As seen from Fig. 4 the measurements of the dilation scale at $z = 0.35$ do not put tight constraints on parameters of the model. At higher redshifts the constrains will be tighter, thus the analysis of the BAO within the backreaction model will be required when future observational data is available. The likelihood function for the BAO has the following form

$$L_{BAO}(\Omega_m, n, h) \propto \exp\left[-\frac{(D_V^{\rm theor} - D_V^{\rm obs})^2}{2\sigma^2_{BAO}}\right]. \tag{19}$$

We assume a flat prior PDF for the parameters within the ranges described above. The 68% and 95% contours of the posterior PDF (marginalized over h and $\Omega_b h^2$) for the joint constraints from the supernovae, CMB and BAO data (with the likelihood function of the following form $L = L_{SN} L_{CMB} L_{BAO}$) are presented in Fig. 4.

The posterior PDF mode is: $\Omega_m = 0.40$, $n = 1.48$, $h = 0.73$, $\Omega_b h^2 = 0.0223$ for the SNLS+CMB+BAO data set and $\Omega_m = 0.42$, $n = 1.14$, $h = 0.72$, $\Omega_b h^2 = 0.0223$ for the Union+CMB+BAO data set. The mean of the marginal posterior PDF for the given parameters (presented in Fig. 5), together with the 68% credible interval are presented in Table 1 and Table 2 for SNLS+CMB+BAO and Union+CMB+BAO respectively.

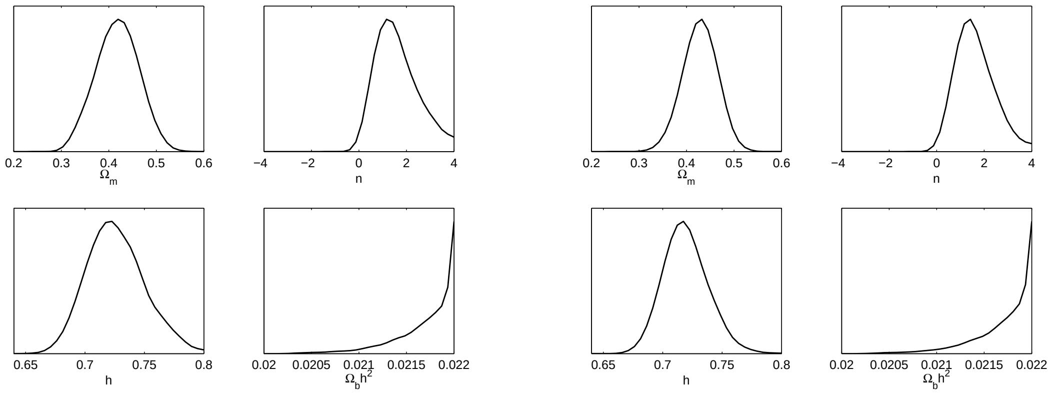

Figure 5. Marginal posterior PDF for model parameters (SNLS+CMB+BAO - left panel, Union+CMB+BAO - right panel).

Table 2. Mean of the marginal posterior PDF for the model parameters together with the 68% credible interval for the SNIa+CMB and SNIa+CMB+BAO data sets.

	Union+CMB	Union+CMB+BAO
Ω_m	$0.40^{+0.04}_{-0.05}$	$0.43^{+0.03}_{-0.04}$
n	$1.02^{+0.79}_{-0.77}$	$1.60^{+0.80}_{-0.76}$
h	$0.74^{+0.03}_{-0.03}$	$0.72^{+0.02}_{-0.02}$
$\Omega_b h^2$	$0.0219^{+0.0003}_{-0.0003}$	$0.0219^{+0.0003}_{-0.0003}$

3.2. Models comparison

3.2.1. ΛCDM vs the backreaction model

In this section we present the comparison between the model considered above (which will be referred to as model 1) and the standard cosmological model - ΛCDM model (which will be referred to as model 0). In the Bayesian framework, models are compared not only by their goodness of fit to the data but also by their complexity (see [25] for a review). The best model from the set of models under consideration is the one with the greatest value of the probability in the light of data defined as

$$P(M_i|D) = \frac{P(D|M_i)P(M_i)}{P(D)}, \tag{20}$$

where M_i is a model under consideration, $P(M_i)$ is the prior probability of a model. If we have no foundation to favour one model over another one from the set of models under consideration we usually assume the same value of the prior quantity for all models, i.e. $P(M_i) = 1/K$, where K is the number of models. $P(D)$ is the normalization constant. $P(D|M_i)$ is called the marginal likelihood (or the evidence) and has the following form

$$P(D|M_i) = \int L(\bar{\theta})P(\bar{\theta}|M_i)\mathrm{d}\bar{\theta} \equiv E_i. \tag{21}$$

It is convenient to consider the ratio of posterior probabilities for the models which we

Table 3. Values of logarithm of the Bayes Factor $\ln B_{ij}$ calculated for the model indexed by i and model indexed by j for different data sets.

Data set	$\ln B_{01}$	$\ln B_{21}$	$\ln B_{02}$	$\ln B_{03}$	$\ln B_{31}$	$\ln B_{04}$	$\ln B_{41}$
SNLS	0.89	−0.22	1.11	1.15	−0.25	1.06	−0.17
Union	0.48	−0.13	0.61	0.74	−0.26	−0.69	−0.21
SNLS+CMB	5.52	3.78	1.74	1.73	3.79	1.87	3.65
Union+CMB	4.94	3.28	1.66	1.59	3.34	1.73	3.21
SNLS+CMB+BAO	4.77	3.13	1.64	1.83	2.93	1.78	2.99
Union+CMB+BAO	4.23	2.58	1.65	1.66	2.57	1.80	2.43

want to compare. If prior probabilities for those models are equal then the posterior ratio reduces to the ratio of the evidences. This ratio is called the Bayes Factor ($B_{ij} \equiv E_i/E_j$). The values of B_{ij} are interpreted as follows: $0 < \ln B_{ij} < 1$ as inconclusive, $1 < \ln B_{ij} < 2.5$ as weak, $2.5 < \ln B_{ij} < 5$ as moderate and $\ln B_{ij} > 5$ as strong evidence in favour of a model indexed by i with respect to a model indexed by j. The evidence [eq. (21)] was calculated using the CosmoNest code. In addition we assumed equal values of the prior probabilities for all considered models and the prior PDF for the model parameters. The values of logarithm of the Bayes Factor calculated for the ΛCDM model (model 0) vs model 1 (i.e. the model presented in Sec. 3.1) – B_{21} – are presented in Table 3.

As one can conclude the comparison in the light of the supernovae data does not give conclusive results, this data set has not enough information to favour one model over another one. After inclusion an information coming from the CMB there is strong (SNLS+CMB) and almost strong (Union+CMB) evidence in favour of the ΛCDM model over the inhomogeneous one. When we include information coming from the BAO the values of the Bayes Factor become smaller in both cases and the evidence to favour the ΛCDM model is moderate.

3.2.2. Relation between the average curvature and the curvature index

In the preceding subsection we could see that the Bayesian method of model comparison prefers the ΛCDM model over the backreaction model. We should be aware that the backreaction model – model 1 – is based on the assumptions (9) and (10). If these assumptions are changed it is possible to obtain a better fit. Below we present models where the assumption (10) is replaced with:

- model 2

$$k(z) = 0. \tag{22}$$

We emphasize that $k = 0$ comes from modification of the assumption (10) only. It is not the same as assuming that $\langle \mathcal{R} \rangle = 0$. As seen from (5) the assumption of

$\langle \mathcal{R} \rangle = 0$ leads to $\mathcal{Q} \sim a^{-6}$, which means that the backreaction is strong in the early Universe and its value decreases with time.
The results of the model comparison are presented in Table 3. As can be seen, both for the SNIa+CMB and SNIa+CMB+BAO data sets, there is moderate evidence to favour the backreaction model with $k = 0$ over the model with relation (10) Note that there is only weak evidence to favour the ΛCDM model over model 2.

- model 3
$$k(z) = -\frac{1}{p}(1+z)^{-(n+2)}. \tag{23}$$
We assume a flat prior PDF for the additional parameter in the range $p \in [0, 100]$. As we could see, model 2 fit observations better than model 1. If indeed $k = 0$ is favoured then we should obtain that the best model with k given by (23) is the one with $p = 100$. However, this is not the case, and as seen from the left panel of Fig. 6 the marginal posterior PDF is almost flat in a very wide range – there is only a little difference between $p = 100$ and the best-fit value. The posterior PDF mode for model 3 is: $\Omega_m = 0.20, n = -0.37, h = 0.78, \Omega_b h^2 = 0.0222, p = 75.80$ (SNLS+CMB), $\Omega_m = 0.20, n = -0.53, h = 0.77, \Omega_b h^2 = 0.0221, p = 50.23$ (Union+CMB), $\Omega_m = 0.27, n = -0.20, h = 0.74, \Omega_b h^2 = 0.0221, p = 63.71$ (SNLS+CMB+BAO), $\Omega_m = 0.31, n = 0.16, h = 0.73, \Omega_b h^2 = 0.0223, p = 48.61$ (Union+CMB+BAO). The means of the marginal posterior PDF for the model parameters are presented in Table 4. The values of logarithm of the Bayes Factor calculated for the ΛCDM model and model 3 ($\ln B_{03}$) as well as for model 3 and model 1 ($\ln B_{31}$) are compared in Table 3. As one can conclude there is weak evidence to favour the ΛCDM model over model 3 and moderate evidence in favour of model 3 over model 1 (for SNIa+CMB and SNIa+CMB+BAO data sets).
- model 4
$$k(z) = -(1+z)^{-(n+2+m)}. \tag{24}$$
We assume a flat prior PDF for the additional parameter in the range $m \in [0, 5]$. The posterior PDF mode for model 4 is: $\Omega_m = 0.20, n = -0.58, h = 0.77, \Omega_b h^2 = 0.0220, p = 3.05$ (SNLS+CMB), $\Omega_m = 0.23, n = -0.56, h = 0.75, \Omega_b h^2 = 0.0222, m = 3.79$ (Union+CMB), $\Omega_m = 0.25, n = -0.37, h = 0.75, \Omega_b h^2 = 0.0221, m = 3.18$ (SNLS+CMB+BAO), $\Omega_m = 0.26, n = -0.38, h = 0.74, \Omega_b h^2 = 0.0220, m = 3.61$ (Union+CMB+BAO). The marginal posterior PDF for the parameter m is presented in the right panel of Fig. 6. The means of the marginal posterior PDF for the model parameters are presented in Table 5. The values of logarithm of the Bayes Factor calculated for the ΛCDM model and model 4 ($\ln B_{04}$) as well as for model 4 and model 1 ($\ln B_{41}$) are compared in Table 3.

These above results are encouraging and motivate further study of the backreaction models. Especially, it is important to study other assumptions than (9) and (10). As seen, if only assumption (10) was modified (models 2-4) then not only we obtained a better fit but also the value of Ω_m realistically decreased compared to model 1.

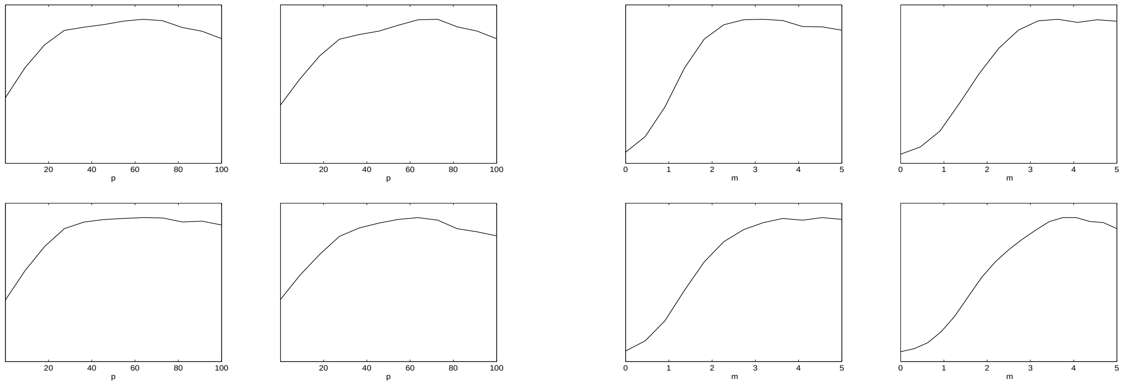

Figure 6. Marginal posterior PDF for the parameter p of model 3 (left panel) and for the parameter m of model 4 (right panel). The upper figures are based on the SNLS+CMB (first and third) and SNLS+CMB+BAO data (second and fourth). The lower figures are based on the Union+CMB (first and third) and Union+CMB+BAO data (second and fourth).

Table 4. Mean of the marginal posterior PDF for the parameters of model 4 together with the 68% credible interval for the SNIa+CMB and SNIa+CMB+BAO data sets.

	SNLS+CMB	SNLS+CMB+BAO	Union+CMB	Union+CMB+BAO
Ω_m	$0.24^{+0.04}_{-0.03}$	$0.28^{+0.06}_{-0.05}$	$0.26^{+0.05}_{-0.05}$	$0.31^{+0.06}_{-0.07}$
n	$-0.18^{+0.28}_{-0.33}$	$0.10^{+0.54}_{-0.55}$	$-0.13^{+0.37}_{-0.41}$	$0.27^{+0.70}_{-0.67}$
h	$0.76^{+0.02}_{-0.02}$	$0.74^{+0.02}_{-0.02}$	$0.75^{+0.02}_{-0.02}$	$0.73^{+0.02}_{-0.02}$
$\Omega_b h^2$	$0.0216^{+0.0005}_{-0.0005}$	$0.0216^{+0.0005}_{-0.0006}$	$0.0216^{+0.0005}_{-0.0006}$	$0.0217^{+0.0005}_{-0.0006}$
p	$53.18^{+30.63}_{-31.26}$	$54.25^{+30.09}_{-31.01}$	$53.99^{+30.97}_{-31.19}$	$53.87^{+30.26}_{-30.43}$

Table 5. Mean of the marginal posterior PDF for the parameters of model 5 together with the 68% credible interval for the SNIa+CMB and SNIa+CMB+BAO data sets.

	SNLS+CMB	SNLS+CMB+BAO	Union+CMB	Union+CMB+BAO
Ω_m	$0.24^{+0.04}_{-0.03}$	$0.28^{+0.06}_{-0.06}$	$0.26^{+0.05}_{-0.05}$	$0.30^{+0.07}_{-0.06}$
n	$-0.32^{+0.29}_{-0.34}$	$-0.06^{+0.52}_{-0.54}$	$-0.26^{+0.40}_{-0.40}$	$0.07^{+0.69}_{-0.65}$
h	$0.76^{+0.02}_{-0.03}$	$0.74^{+0.02}_{-0.02}$	$0.74^{+0.02}_{-0.02}$	$0.73^{+0.02}_{-0.02}$
$\Omega_b h^2$	$0.0216^{+0.0005}_{-0.0006}$	$0.0216^{+0.0005}_{-0.0006}$	$0.0216^{+0.0005}_{-0.0006}$	$0.0216^{+0.0005}_{-0.0006}$
m	$3.00^{+1.34}_{-1.31}$	$3.20^{+1.23}_{-1.22}$	$3.13^{+1.29}_{-1.28}$	$3.22^{+1.22}_{-1.24}$

4. Conclusions

In this paper we presented the Bayesian analysis of the backreaction models. This work was motivated by the recently proposed model of the inhomogeneous alternative to dark energy [10]. In this approach the Universe is modelled by the Buchert equations, which describe the relations between the scale factor, the average spatial curvature, average matter distribution, average expansion and shear. Larena et al. [10] showed that their model is consistent with supernova and CMB data. Here we included the BAO data and tested this model within the Bayesian approach.

Our analysis shows that the SNLS and CMB data alone strongly favours the ΛCDM model. With Union sample and BAO data there is almost strong evidence ($\ln B_{21} > 4$) to favour the ΛCDM over the backreaction model. However, if just the best-fit models are compered, then the χ^2 (Union+CMB+BAO) for the ΛCDM and model 1 are 320.96 and 325.36 respectively. If the χ^2 distribution is assumed then for 307 numbers of degree of freedom for model 1 the probability that this model is true in the light of data is 22.6%. For comparison for the ΛCDM (308 degree of freedom) we get 29.3%. So we can see that the best-fit model 1 fits observations almost as good as the ΛCDM model. Still there are some other concerns regarding this model. For example, can the assumptions (9) and (10) be justified? In other words, how does the backreaction and the spatial curvature of the real Universe evolve, and does the relation $\mathcal{Q} \sim \langle \mathcal{R} \rangle$ for the real Universe hold? Even still, the most concerning is the value of Ω_m, which is quite large, $0.43^{+0.03}_{-0.04}$. However, as it was shown in Sec. 3.2.2, after the assumption (10) was modified, we were able to obtain a better fit and, in addition, the value of Ω_m decreased to $0.31^{+0.06}_{-0.07}$ and $0.30^{+0.07}_{-0.06}$ (or even lower if the BAO data is excluded – see Tables 4 and 5) for model 4 and 5 respectively. This shows, that still a lot needs to be done in the context of the backreaction models, especially in the study of the relation between the average spatial curvature and the backreaction. Currently the ΛCDM model is preferred by the observational data but it is possible that after the revision of assumptions (9) and (10) we can obtain a more satisfactory fit. We should also remember that among different models of dark energy, here, the dark-energy-term appears as a consequence of inhomogeneities that are present in the Universe. Therefore, within this class of models the "decaying lambda term" reveals a new and natural interpretation.

Acknowledgments

This research was supported by the Peter and Patricia Gruber Foundation and the International Astronomical Union (KB) and by Marie Curie Host Fellowships for the Transfer of Knowledge project COCOS (Contract No. MTKD-CT-2004-517186) (AK, MS).

References

[1] Koyama K 2008 *Gen. Rel. Grav.* **40** 421

[2] Capozziello S and Francaviglia M 2008 *Gen. Rel. Grav.* **40** 357
[3] Célérier M N 2007 *New Adv. Phys.* **1** 29
[4] Krasiński A 1997 *Inhomogeneous Cosmological Models* (Cambridge: Cambridge University Press)
[5] Stephani H, Kramer D, MacCallum M, Hoenselaers C and Herlt E 2003 *Exact solutions of Einstein's field equations* 2nd edition (Cambridge: Cambridge University Press)
[6] Buchert T 2000 *Gen. Rel. Grav.* **32** 105
[7] Räsänen S 2006 *J. Cosmol. Astropart. Phys.* JCAP11(2006)003
[8] Buchert T 2008 *Gen. Rel. Grav.* **40** 467
[9] Buchert T and Carfora M 2008 *Class. Quant. Grav.* **25** 195001
[10] Larena J, Alimi J-M, Buchert T, Kunz M and Corasaniti P-S 2008 *Preprint* arXiv:0808.1161
[11] Buchert T, Larena J and Alimi J-M 2006 *Class. Q. Grav.* **23** 6379
[12] Paranjape A and Singh T P 2008 *Gen. Rel. Grav.* **40** 139
[13] Räsänen S 2006 2007 *Preprint* arXiv:0705.2992
[14] Jeffreys H 1961 *Theory of Probability* (Oxford: Oxford University Press)
[15] Mukherjee P, Parkinson D and Liddle A R 2006 *Astrophys. J.* **L51** 638; code available from http://www.cosmonest.org/
[16] Skilling J 2004 *Bayesian Inference and Maximum Entropy Methods in Science and Engineering* (*AIP Conf. Proc. vol 735 p 395*); http://www.inference.phy.cam.ac.uk/bayesys/
[17] Lewis A and Bridle S 2002 *Phys. Rev.* **D66** 103511; code available from http://cosmologist.info/cosmomc/
[18] Astier P et al. 2008 *Astron. Astrophys.* **447** 31
[19] Kowalski et al. 2008 *Preprint* arXiv:0804.4142
[20] Doran M and Lilley M 2002 *Mon. Not. R. Astron. Soc.* **330** 965
[21] Hinshaw G *et al* 2007 *Astrophys. J. Suppl. Ser.* **170** 288
[22] Hu W and Sugiyama N 1996 *Astrophys. J.* **471** 542
[23] Freedman W L et al. 2001 *Astrophys. J.* **553** 47
[24] Pettini M et al. arXiv:0805.0594
[25] Trotta R 2008 *Contemporary Physics* **49** 71